Journal of Physical Chemistry and Functional Materials

Home Page of Journal: https://dergipark.org.tr/jphcfum

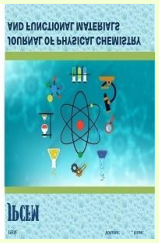

Theoretical Calculations and Spectroscopic Analysis of Gaussian Computational Examination-NMR, FTIR, UV-Visible, MEP on 2,4,6-Nitrophenol

Dyari Mustafa MAMAND [a,b,*]

[a] *University of Raparin, College of Science, Department of Physics, Sulaimaneyah, Iraq*

[b] *Firat Universityt, Faculty of Science, Department of Physics, Elazig Turkey*

ABSTRACT

Quantum computational is a significant method to explain and investigation the electronic construction (ground state basically) of many-body systems, in particular atoms, molecules, and the condensed phases. by utilizing the functional can describe characteristics of a many-electron scheme. At this study quantum, computational measurements are applied by used density functional theory (B3LYP) and Hartree-Fock approximation including 6-311G basis sets the identical sequences are analyzed. The interchange of the composition of nitrophenol due to the consequent replacements of NO2 is examined. A study on the electronic properties; absorption wavelengths, excitation energy, dipole moment and frontier molecular orbital energies, are performed by HF and DFT methods. The calculated HOMO and LUMO energies. Besides frontier molecular orbitals (FMO), molecular electrostatic potential (MEP) was performed. The thermodynamic properties (thermal energy, heat capacity and entropy) of the title compound are calculated and are interpreted with phenol.

ARTICLE INFO

Keywords:

2,4,6-Nitrophenol
Vibrational sequence pattern
FTIR
NMR
UV-vis
Frontier molecular orbital energies
Electrostatic potential map

Revised: 12-November-2019,
Accepted: 06-December-2019
ISSN: 2651-3080

1. Introduction

The aromatic arrangements in conjugated with the nitro group starting to energies transference, methods have been deeply analyzed and their crystals are extremely understood approximately the substances of the expectation, because their molecular universe joined with the versatility of artificial chemistry can be applied to reconstruct their construction to maximize the non-linear characteristics with attention to artificial fabrication [1, 2]. The nitro substituted phenols with large optical nonlinearities are very encouraging matters for ultimate optoelectronic and non-linear optical utilization. The visual transparency of the crystal is, considerably great and consequently, it can hold a potential component for frequency replication in electro-optic modulation, frequency reduction and THz wave reproduction of non-linear optics [3, 4].

Phenol has a great chemical structure, are attractive molecules for academic investigation, because of their comparatively tiny size and relationship to biological varieties. The type compound of phenols is organic compounds that include a hydroxyl gathering directly bonded to a carbon atom in the ring of benzene. The phenol substances, including extremely high second-order nonlinear optical susceptive, should drag a lot of concentration because of their potential applicability in electro-optic modulation. phenols material is very interest chemical material with added nitro group possessing the characteristics of high second-order optical nonlinearities. Small transparency cut-off wavelength and thermal stability show which, is required in the accomplishment of the greatest of the modern electronic

* Corresponding author:
E-mail (diyarimustafa47@gmail.com)

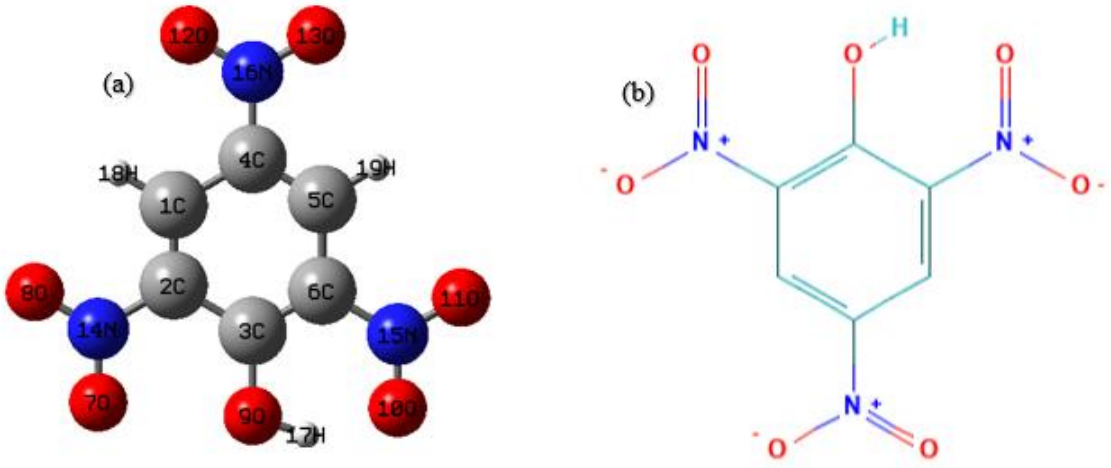

Figure 1. 2,4,6-Trinitrophenol (a) fully optimized, (b) $C_{16}H_{11}N_3O_7$ chemical structure.

Table 1. HF and DFT calculations vibrational frequencies of 2,4,6-Nitrophenol. S – Strong; as-Asymmetric; s – symmetric; δ- In plane bending; γ– out plane bending; τ – Twisting

S.NO	Observed Frequency(cm^{-1}) FTIR		Vibrational Assignments	S.NO	Observed Frequency(cm^{-1}) FTIR		Vibrational Assignments
	HF 6-311G	DFT 6-311G			HF 6-311G	DFT 6-311G	
1	38.18	50.62	(O-H) U	27	829.01	803.38	(NO2) δ
2	63.88	53.96	(C-H) U	28	875.81	820.54	(NO2) δ
3	80.18	60.98	(C-H) U	29	935.96	902.99	(CCC) *δ*
4	115.93	96.38	(C=C) U	30	972.47	938.66	(CCC) *δ*
5	165.94	126.34	(C=C) U	31	1015.70	999.02	(CCC) *δ*
6	198.39	151.70	(C=C) U	32	1087.85	1015.77	(C-N) *δ*
7	209.11	181.73	(N-O) U as	33	1110.09	1112.61	(C-N) *δ*
8	267.11	198.76	(N-O) U as	34	1129.90	1187.98	(C-N) *δ*
9	318.53	314.37	(N-O) US	35	1173.07	1195.33	(NO_2) γ
10	339.94	322.76	(C-C) U	36	1207.43	1236.72	(NO_2) γ
11	345.29	339.78	(C-C) U	37	1377.07	1274.06	(NO_2) γ
12	383.93	351.47	(C-C) U	38	1390.19	1293.41	(CCC) γ
13	430.38	389.26	(N-O) US	39	1406.97	1297.08	(CCC) γ
14	483.49	400.55	(N-O) US	40	1415.44	1344.85	(CCC) γ
15	501.79	447.74	(N-O) US	41	1426.45	1408.23	(C-O) *δ*
16	549.76	512.18	(O-H) δ	42	1430.78	1426.24	(C-N) *γ*
17	557.46	542.05	(C-H) δ	43	1476.47	1443.24	(C-N) γ
18	616.61	548.67	(C-H) δ	44	1532.18	1472.39	(C-N) γ
19	675.18	641.99	(C-N) U	45	1542.86	1498.53	(C-O) γ
20	701.25	681.91	(C-N) U	46	1649.32	1552.15	(C-N) γ
21	709.91	695.27	(C-N) U	47	1741.57	1623.03	(C-N) γ
22	767.46	702.80	(C-O) U	48	1756.57	1658.28	(C-OH) τ
23	782.93	713.67	(C-H) γ	49	3390.59	3242.03	NO_2 τ
24	797.38	727.39	(C-H) γ	50	3391.87	3243.11	NO_2 τ
25	801.62	763.35	(O-H) γ	51	3742.48	3303.44	NO_2 τ
26	805.54	786.88	(NO_2) *δ*				

forms. Transparency in the ultraviolet range and more cost threshold adequately high nonlinear coefficient, the material. The 2,4,6-Trinitrophenol Frequently recognized as picric acid because of the smaller cutoff wavelength is a nonlinear optical crystal also a famous organic crystal [5]. TNP is a popular material utilized in the dyeing manufacturers [5]. NLO materials, which can generate highly efficient second-harmonic blue-violet are of great

interest for various applications including optical communication, optical computing, optical information processing, optical disk data storage, laser fusion reactions, laser remote sensing, color display, medical diagnostics, etc [6]. It is also widely used in the dye industry, rocket fuel, fireworks, pharmaceuticals, chemical laboratories [7]. can be used as an excellent probe for fluorescence sensing [8], photocatalysis [9], photoelectrochemical and electrochemiluminescence sensing [10].

2. Computational Calculation

Everything certain computations have been carried out applying GAUSSIAN 09W [11], in personal computer. Hartree-Fock and HF and hybrid approaches; B3LYP are applied utilizing the basis set 6-311G. In DFT methods; Becke's three parameter hybrids function combined with the Lee-Yang-Parr correlation function (B3LYP) [12, 13] Becke's three parameter exact exchange-function (B3) [14] combined with gradient-corrected correlational functional of Lee, Yang and Parr (LYP) [15, 16] and predict the most beneficial consequences for molecular geometry and vibrational frequencies for slightly more comprehensive molecules. The estimated frequencies are estimated down to generate the coherent among the perceived frequencies. Gauss view program is shown the optimized structure of the phenol in Figure 1.

The optimized trinitrophenol molecule is established from Gaussian09. structural parameters such as bond length, bond angle and dihedral angle are obtainable in Table 2. The detected (FT-IR) and considered vibrational frequencies and vibrational assignments are acquiesced in Table 1

The complete computed amounts of B3LYP system are higher than the HF approximation. the TNP structure has three NO2 symmetrical located near 1200 in phenyl ring cause of the breaking of TNP construction relates to various planes. The C-C bond length of the phenyl ring becoming split and fractured variably. It is additionally obvious from the bond length distribution as C6-C3< C1-C2<C3-C2<C5-C6. The elongation bond length of C3-C2 and C5-C6 are greater than other bond lengths of C-C because of the behavior of NO2 gathering.

3. Result and discussion

3.1. Vibrational assignments

Computed the harmonic vibrational frequency, estimated at HF and DFT method. Caparisoned both methods result at quantum computational calculation used GAUSSIAN09. Examined FT-IR for different modes of vibrations have been displayed in Tables 1 and 2. Identification of frequencies measured at HF and B3LYP.

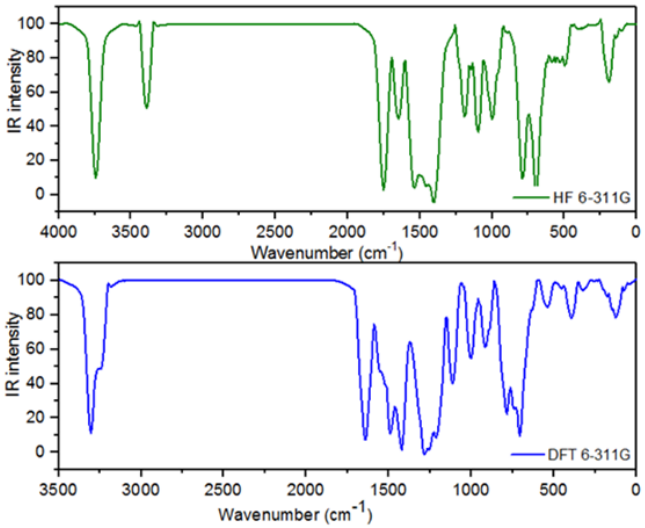

Figure 2. Gaussian09 calculations for FT-IR spectra of 2,4,6-Nitrophenol at HF and DFT(B3LYP) with 6-311G basis sets.

C-H vibration: toward clearness, the C-H or C-C vibrations of aromatic composites are examined as a separate ring. however, as including each complicated molecule, vibrational interaction of atoms happens and those designs just show the predominant vibration. Interchanged benzenes have a high quantity of sensitive bands. such are banding whose location is importantly influenced by the mass and electronic characteristics, mesomeric or inductive [17, 18], of the substituents. Because of the stretching interaction vibrations of the ring CIH bonds, appear four or three peaks at some polynuclear and mononuclear aromatic compositions at the range (3000-3100) cm-1 in the infrared spectra field [19]. Consequently, in the existing investigation, the stretching vibration of C-H is three and noticed at 3746 and 3306.42 cm-1. Those indicated frequencies are downshifted to the recognized field which strongly shows that the ring vibrations influenced enormously by the replacements. out-of-plane with in-plane of the C-H bending vibrations usually recline and lie in the plain 950 - 800 cm-1 and 1000-1300 cm-1 [20, 21] sequentially. In-plane bending vibrations are observed at 1150 and 1180 cm-1 of three C-H vibrations but for out-plane bending vibrations are detected at low range than in-plane at 1183 and 1093 cm-1. Associated with the article the out-plane and in-plane bending vibrational frequencies are determined to imply properly inside their particular areas.

C-C vibrations: The general region of C-C stretching vibration in aromatic compositions are observed in the range 1430-1650 cm-1 [22, 23]. but the stretching vibrations of tetraphenyl are recognized at a region at 1645, 1543 cm-1 exhibit quite strong intensity to C=C vibrations. But the single bond amongst carbons has a lower intensity

and indicated in the range at 1402, 1490 cm-1. All bands lie in the below edge of the normal region while corresponding to the record amounts. The CCC out-plane bending vibration is detected at region 393, 490 cm-1, but the in-plane bending vibrational possess seemed at range 797, 714 cm-1. These distributions are in the excellent arrangement among the research [24].

NO2 vibrations: Due to strong absorption of nitro composition and aromatic compound have symmetric with asymmetric stretching vibration of the gathering NO2 at range 1282-1196 and 1536 -1501 cm-1sequentially, but the Hydrogen influence bond is very little on the NO2 group asymmetric stretching vibration [25, 26]. A very strong band of NO2 should be specified to symmetric and asymmetric stretching modes at region 1536 and 1489 cm-1 and 1422, 1287 cm-1. Every one of TNP stretching vibration is rundown of the exacted range. this arrangement of the stretching vibration restores to inductive influence H of Phenol and O of NO2. The band of the nitro composite is weak to medium intensity the range between 590 – 500 cm-1 [27] because of deformations mode of NO2 gathering the out of plane bending deformations form. the strong intensity was detected at region 538 and 400 cm-1 for the title composite. in the range, 775-660 cm-1 [28, 29] specified deformation vibration of the NO2 at the in-plane and appear weak to medium absorption. In the existing situation, the NO2 deformation mode is located in 789-707 cm-1. The twisting vibration of NO2 is detected at region 125 cm-1.

C-N vibrations: The C-N stretching vibrations appeared the peaks at the high region of 350-1000 cm-1 [30]. but the C-N stretching vibrations is smaller than this range and detected at 1090, 1107 and 991 cm-1. the nitro gathering bending vibrations of C-N occur approximately 610 and 870 cm-1 [31]. At the in-plane bending indicated at 694 cm-1, correspondingly of the title composite. Out-plane bending vibrations of the C-N are detected at range 328, 173 cm-1. Some of the indicated amounts of C-N bending vibrations and stretching are perceived at out of the expected range. the wavenumber of the normal mode of vibrations was decreased because due to the repulsion and has an opposite relation at this present study due to the NO2 repulsions.

C-O and O-H vibrations: The carbonyl group is another group in TNP, this group has very strong stretching due to the C-O band and absorption produced by it [32]. The attention of those parts begins to designate a band perceived stretching vibration at the region 911 cm-1 to C-O stretching vibration. the out-plane and in-plane bending vibration arrive at the region 125 cm-1 and 328 cm-1 sequentially. Furthermore, a weak band is seen at 125 cm-1 for C-OH twisting vibration. From the above consideration, it is obvious that the detailed band is in the assumed range [33] and great agreement with estimated conditions at B3LYP/6-311G. The OH gathering produce an addition to three different vibrations, out of plane bending vibrations, in-plane bending and stretching. The OH group vibrations are possible to be the usual sense to the environment, so both appearances declared shifts in the spectra of the H-bonded species. the H-bonding are very susceptible to O-H stretching, this stretching detected near 3300 cm-1 [34]. Consequently, in TNP, the O-H stretching is observed at the region 3300 cm-1. The O-H out-of-plane and in-plane bending vibrations are normally recognized in the ranges 720-590 cm-1 and 1350-1200 cm-1 [35, 36] sequentially. The O-H out-plane bending vibrations and in-plane bending vibrations are detected at 782 cm-1 and 1121 cm-1 sequentially. Without one, the assignment is in the range including the literature. The out of plane bending vibration is turned and shifted up to the bigger range which is perhaps favor of NO2.

3.2. NMR investigation on TNP

Nuclear magnetic spectroscopy is currently utilized for construction explanation of organic molecules. The optimized molecule was utilized to the NMR spectra at HF and B3LYP level of DFT with 6-311G basis set. The chemical shifts of the composite are described in ppm for NMR spectra which are displayed in Tables 3. Given the range of NMR chemical shifts for comparable organic molecules normally are >100 ppm [36, 37], the correctness assures certain description of spectroscopic parameters. Because of entire 2,4,6-Nitrophenol has three nitro group and it was added into the phenyl ring. The electronegativity of N atom is very large due to this characteristic the electrons distributions are polarized in its bond to a neighboring carbon atom and therefore raises the chemical shift of C1, C2, C4 and C6 (53.23, 40.65, 43.20and 45.24 and 46.51, 49.87, 47.97, 54.42) ppm for DFT and HF sequentially.

The substitution of OH and NO2 on C2, C2, C6 was exist caused by rising shift more than others shifts in the ring. The substitution of NO2 makes rising the chemical shift of C1, C2 and C3 in the phenyl ring and due to the breaking of proton shield. The substitution of NO2 has an influence on the shift of other C in the ring fluctuates related to the states of the NO2. The chemical shifts of carbons are reduced in going from tri-nitro phenol. because of the isolation of O-H bond in the nitro to tri-nitro make the reduce the chemical shift of O of phenol directly (92.43, 31.53, 31.53, 15.3, 2.82). This conclusion of isolation is the principal reason to alter the chemical characteristic of nitrophenol to trinitrophenol. There is no difference from

Table 3. Theoretical NMR calculations for 2,4,6, -Nitrophenol NMR chemical shift (ppm)

Atom position	HF (6-311G) ppm	DFT (6-311G) ppm	Shift
C1	46.51	53.23	6.72
C2	49.87	40.65	9.22
C3	16.8	26.83	10.03
C4	47.97	43.20	4.77
C5	47.74	59.32	11.58
C6	54.42	45.24	9.18
N14	-277.32	-170.49	-106.83
N15	-277	-168.10	-108.9
N16	-276.56	-164.64	-111.92
O7	-676.66	-584.23	-92.43
O8	-507.63	-539.16	-31.53
O9	175.62	160.32	15.3
O10	-410.13	-412.95	-2.82
O11	-601.03	-520.29	8-0.74
O12	-559.13	-494.34	-64.79
O13	-525.33	-487.19	-38.2
H17	19.62	20.60	0.98
H18	22.42	23.48	1.06
H19	22.63	23.38	0.75

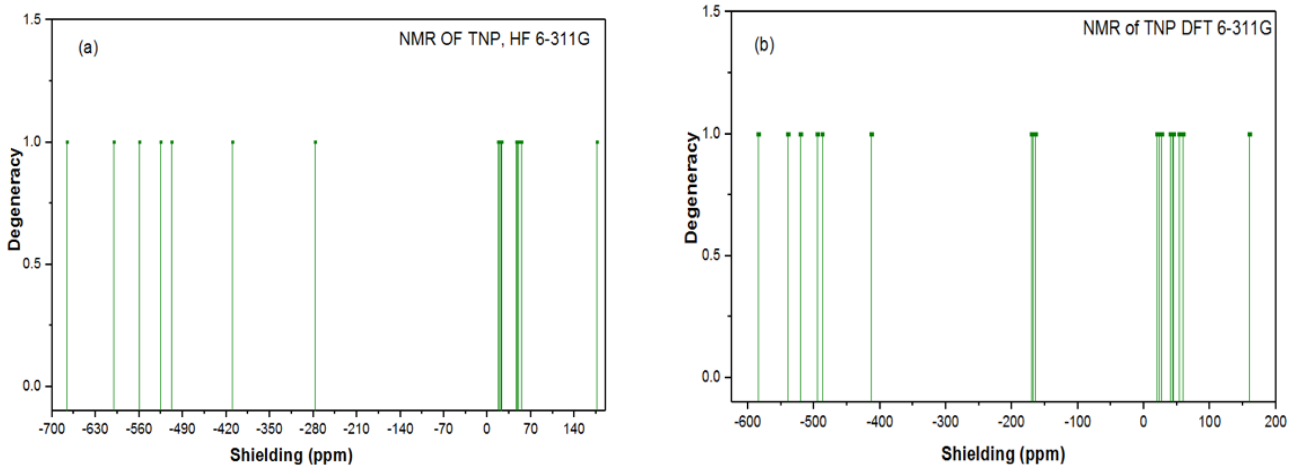

Figure 3. NMR spectrum of TNP molecule (a)HF and (b) DFT for 6-311G basis set.

the chemical shift in N and O among three phenols. This illustration explicates that the rigidity of the diamagnetic shielding of the atom can determine and specify this characteristic. Of the investigation, it is obvious that the change in the chemical characteristic of phenols is particularly in favor of NO2 gatherings. In computing to this, due to the convenience of nitro gatherings, the phenyl ring itself is interrupted. This representation is further confirmation that the complete characteristic of the phenol is diverted towards the specific nitro gathering.

4. Electronic properties-HOMO-LUMO analysis

The electrical and optical property of the organic molecules can determine by using the frontier molecule orbital [38]. The destabilizing of the antibonding of molecule and stabilizing of bonding molecule orbital can increase with increase the overlap of the two orbitals. In the chemical interaction the two outer orbitals of the atoms or molecules are very significant. One of the orbitals represent the donate an electron and have donate ability named HOMO occupied molecular orbital, other orbital is acceptor

orbital and has a lower energy than HOMO low unoccupied molecular orbital represents to accept an electron [39]. Both orbitals sometimes recognized and identified by frontier molecule orbital. The interaction between theses two orbitals are more stable with named filled empty interaction [40].

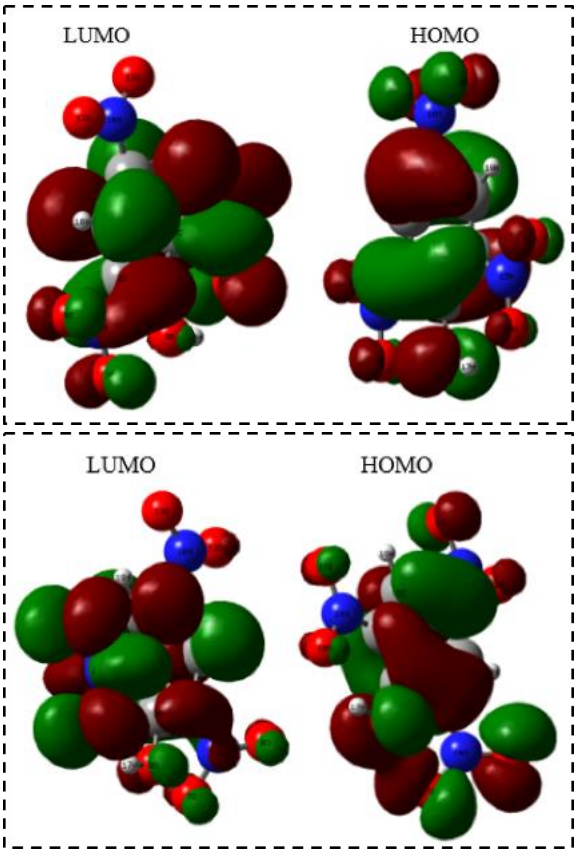

Figure 4. HOMO-LUMO of TNP. (a) HF, (b) DFT at 6-311G basis set

The three-dimensional plot of frontier orbital HOMO and LUMO was shown in figure 5, of TNP. corresponds to this Figure, the HOMO is principally surrounded above three carbons of phenyl ring which combines two NO2 gatherings. Close to NO2 group the SP orbital od oxygen overlapped with (O-H) SP orbital lobe. The charge concentration and distribution of phenyl ring on carbon and Nitrogen of NO2 describe the property of LUMO orbital. Molecule electron density determination control at the range among two nuclei, while the two identical type orbitals overlap to produce a new molecular orbital. The new molecule orbital obtains as a conclusion from in-phase interaction, not out-phase interaction describes the lower energy orbital of bonding orbital than the pristine atomic orbital before interaction. According to higher energy molecular orbital in the out-phase of interaction create the antibonding molecular orbital than the fundamental atomic orbital before interaction and overlaps atomic orbitals. from this study, it is obvious that the out and in of phase orbital interaction are represented LUMO and HOMO sequentially. Electron density transfer indicated at the HOMO to LUMO from NO2 gathering. The HOMO and LUMO energy values for HF approximation is (-11.718 and -0.915) eV respectively. The difference between HOMO and LUMO is bandgap energy of TNP is 10.803 eV. The HOMO and LUMO energy values for DFT method is -8.734 and -4.685 (eV) respectively, the separation between them is band gap energy is 4.049 (eV). The electrical conductivity of the TNP molecule can be expect from the lowering energy gap and speculate the average electrical activity of the TNP molecule.

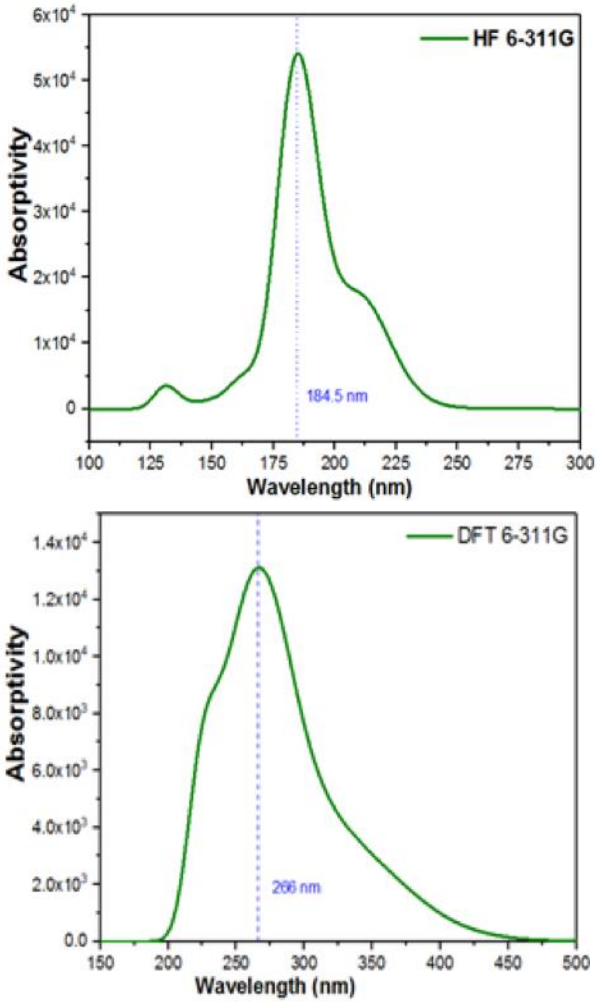

Figure 5. UV-visible spectrum of $C_{16}H_{11}N_3O_7$ (TNP)

4.1. Optical characteristics (HOMO-LUMO interpretation)

For identify the appearance of chromophores in the TNP molecule utilized the UV-visible spectroscopy and for the exhibit, this synthesis has non-linear optical property or not. For optimizing the TNP molecules electron construction in the single state. The electronic excitation in low energy state are estimated at the HF approximation and DFT method at (6-311G level). HF approximation and DFT method calculations indicated just one transition in the invisible region electromagnetic light. The type of basis set

is more important for detecting the accurate peaks and number of peaks in UV-visible calculation.

The one transitions occurred in (185.5 and 266) nm, for each one HF and DFT respectively, assigned to an $n \rightarrow \pi^*$transition. According to this transition of estimate absorption spectra the extreme absorption wavelength resembles to the electronic transition from the HOMO to LUMO with extreme involvement. At this molecule the characteristics was altered from nitro phenol to tri-nitro phenol because of chromophore, the chromophore is NO_2, added NO2 group additional.

Band gap energy correspond to UV-visible spectrum is very significant for explain and exhibiting the chemical property of molecules. From maximum absorption legally can determine the energy gap. At this study have just one peak appeared from the gaussian result of UV-visible spectrum. Associate with HF maximum absorption is (185.5 nm), correspond to this value band gap energy is 6.7 (eV). At DFT method calculation the maximum absorption of energy is 266 nm, the band gap energy of TNP related to this method is 4.67 (eV).

The electronegativity and potential, chemical hardness and Electrophilicity index are estimated and their principles are exposed in Table 4. Can describe the TNP stability associate with the chemical hardness and it is a great indicator with good evidence for defining the capability of TNP of stability ratio. when the valence electron flow from the highest orbital between LUMO acceptor and the HOMO donor can be described by Electrophilicity and is calculate the energy lowering. From the table 4, the Electrophilicity of TNP is (4.083, 10.851) for HF and DFT respectively. this amount assures that the great amount of energy transformation among HOMO and LUMO. The dipole moment is another significant electronic behavior of molecular. The high value of dipole moment indicates and imply to strong interaction. The intermolecular interaction of TNP is not very low Consequently, it is assumed that, the TNP has low intermolecular interactions.

Table 4. Calculated energy values, chemical hardness, electro negativity, Chemical potential and Electrophilicity index of 2,4,6-Nitrophenol in Gas phase from UV-Visible.

HF 6-311G		DFT 6-311G	
E_{HUMO}(eV)	-11.718	E_{HUMO}(eV)	-8.734
E_{LUMO}(eV)	-0.915	E_{LUMO}(eV)	-4.685
$\Delta E_{LUMO-HUMO}$(eV)	10.803	$\Delta E_{LUMO-HUMO}$(eV)	4.049
Chemical hardness (η)	5.415	Chemical hardness (η)	2.074
Electronegativity (χ)	5.4015	Electronegativity (χ)	2.024
Chemical potential (μ)	-6.613	Chemical potential (μ)	-6.709
Chemical softness(S)	0.184	Chemical softness(S)	0.482
Electrophilicity index (ω)	4.038	Electrophilicity index (ω)	10.851
Dipole moment	$6.282*10^{-30}$ Cm	Dipole moment	$5.893*10^{-30}$ Cm

5. Molecular electrostatic potential (MEP) map

Charge distribution of molecules can describe and achieving by electrostatic potential surface This map diagram provides us to imagine variably charged particle zones of molecule surfaces. The advantages of electrostatic potential map are to display the how the chemical interaction occur from the inside of molecule and chemical bonds, can be assume how molecules interact with other molecules by utilizing the charge distribution of the surface of molecules. The electrostatic potential map of TNP was determined according to HF approximation and DFT at 6-311G basis set. Electrostatic map can be defining by color scale. The red color indicates the high electron density and electron distribution on red surface color is very condensate, but the blue color exhibits the lower region of electron density and electro negativity variance is not very great. The charge distribution is difference implies the electronegativity difference, can determine the polarization of the charges. This large electronegativity variation heads to fields that are essentially completely red and most blue. Red region corresponds to great electronegativity and the area of lowest electrostatic potential. The range of color of TNP molecule for dark red (- 0.06948 a.u) and deepest blue range is (- 0.06948 a.u). the negative green range is related to nucleophilic reactivity, the positive range (blue) is related to the electrophilic activity of MEP map. The most positive region is localized on the phenyl group and the bond between Carbon and Nitrogen designating a feasible site for nucleophilic assault. The positive (blue range) appeared on the Oxygen atoms at the edge of the molecule.

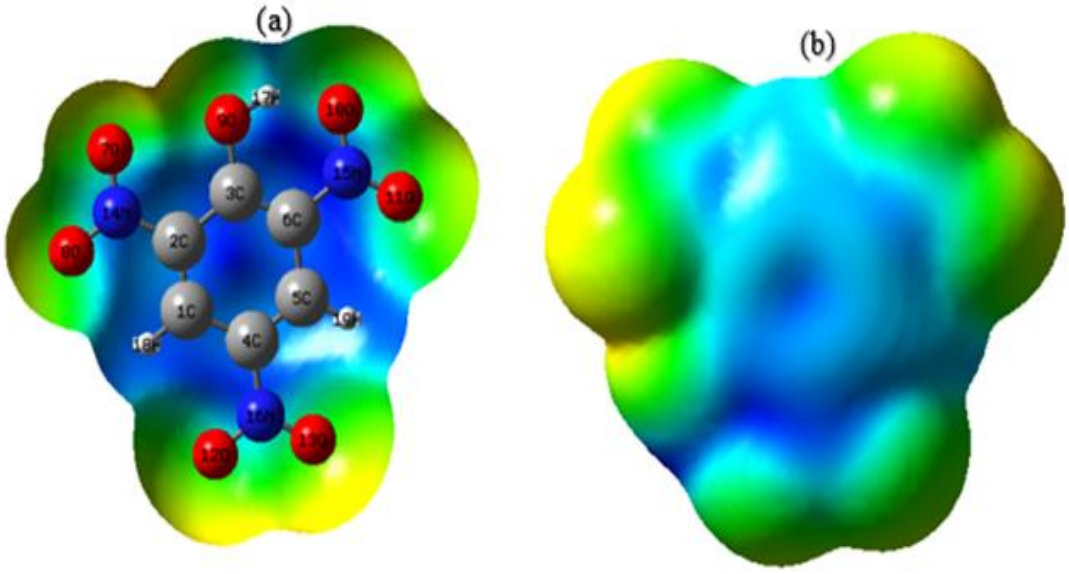

Figure 6. Electrostatic potential map of TNP (a) HF 6-311G (b)DFT 6-311G

The positive potential positions demonstrated by MEP around the carbon and near Nitrogen as well as negative potential positions appeared on an electronegative atom or Oxygen atom. corresponds to these calculations, exhibits the O atom has a strong repulsion as well as it is obvious carbon and Nitrogen provide the strong attraction.

6. Conclusion

In this theoretical investigation, calculated to FTIR of 2,4,6-Nitrphenol molecule by applied the HF and DFT method at 6-311G. the detected vibrational frequencies were specified depending upon their expected range. Compared the value of Bond angles, bond lengths and dihedral angles of TNP molecule between DFT method and HF approximation. Also calculated to NMR associated theoretically corresponds to HF and DFT and detected the shifts of atoms. Explained the optical and electrical properties by calculated the value of HOMO and LUMO. From UV-visible spectroscopy demonstrated that the occurring of charge transformation within the molecule. The electrostatic potential map was applied and determined the distribution of electrons on the molecules surface.

References

[1] Kajzar, F. (1987). Nonlinear optical properties of organic molecules and crystals, *Cubic Effects in Polydiacetylene Solutions and Films*, C 2.

[2] Arivazhagan, M. and Jeyavijayan, S. (2011). Vibrational spectroscopic, first-order hyperpolarizability and HOMO, LUMO studies of 1, 2-dichloro-4-nitrobenzene based on Hartree–Fock and DFT calculations, *Spectrochimica Acta Part A: Molecular and Biomolecular Spectroscopy*, C 79, 376-383.

[3] Schneider, A., Neis, M., Stillhart, M., Ruiz, B., Khan, R.U., and Günter, P. (2006). Generation of terahertz pulses through optical rectification in organic DAST crystals: theory and experiment, *JOSA B*, C 23, 1822-1835.

[4] Ferguson, B. and Zhang, X.-C. (2002). Materials for terahertz science and technology, *Nature materials*, C 1, 26.

[5] Srinivasan, P., Gunasekaran, M., Kanagasekaran, T., Gopalakrishnan, R., and Ramasamy, P. (2006). 2, 4, 6-trinitrophenol (TNP): An organic material for nonlinear optical (NLO) applications, *Journal of crystal growth*, C 289, 639-646.

[6] Pal, T., Kar, T., Bocelli, G., and Rigi, L. (2004). Morphology, crystal structure, and thermal and spectral studies of semiorganic nonlinear optical crystal LAHClBr, *Crystal growth & design*, C 4, 743-747.

[7] Han, Y., Chen, Y., Feng, J., Liu, J., Ma, S., and Chen, X. (2017). One-pot synthesis of fluorescent silicon nanoparticles for sensitive and selective determination of 2, 4, 6-trinitrophenol in aqueous solution, *Analytical chemistry*, C 89, 3001-3008.

[8] Kaur, M., Mehta, S.K., and Kansal, S.K. (2017). Nitrogen doped graphene quantum dots: Efficient fluorescent chemosensor for the selective and sensitive detection of 2, 4, 6-trinitrophenol,

Sensors and Actuators B: Chemical, C 245, 938-945.

[9] Qu, D., Zheng, M., Du, P., Zhou, Y., Zhang, L., Li, D., Tan, H., Zhao, Z., Xie, Z., and Sun, Z. (2013). Highly luminescent S, N co-doped graphene quantum dots with broad visible absorption bands for visible light photocatalysts, *Nanoscale*, C 5, 12272-12277.

[10] Yan, Y., Liu, Q., Du, X., Qian, J., Mao, H., and Wang, K. (2015). Visible light photoelectrochemical sensor for ultrasensitive determination of dopamine based on synergistic effect of graphene quantum dots and TiO2 nanoparticles, *Analytica chimica acta*, C 853, 258-264.

[11] Frisch, M.J., Trucks, G., Schlegel, H., Scuseria, G., Robb, M., Cheeseman, J., Scalmani, G., Barone, V., Mennucci, B., and Petersson, G. (2009). Gaussian 09, Revision D. 01, Gaussian, *Inc.: Wallingford, CT*, C.

[12] Zhou, Z., Du, D., Xing, Y., and Khan, S. (2000). Calculation of the energy of activation in the electron transfer reaction not involving the bond rupture at the electrode, *Journal of Molecular Structure: THEOCHEM*, C 505, 247-255.

[13] Zhou, Z., Fu, A., and Du, D. (2000). Studies on density functional theory for the electron-transfer reaction mechanism between M–C6H6 and M+–C6H6 complexes in the gas phase, *International Journal of Quantum Chemistry*, C 78, 186-194.

[14] Becke, A.D. (1988). Density-functional exchange-energy approximation with correct asymptotic behavior, *Physical review A*, C 38, 3098.

[15] Lee, C., Yang, W., and Parr, R.G. (1988). Development of the Colle-Salvetti correlation-energy formula into a functional of the electron density, *Physical review B*, C 37, 785.

[16] Becke, A., (2007). *The quantum theory of atoms in molecules: from solid state to DNA and drug design*, John Wiley & Sons,

[17] Socrates, G., (2004). *Infrared and Raman characteristic group frequencies: tables and charts*, John Wiley & Sons,

[18] Eazhilarasi, G., Nagalakshmi, R., and Krishnakumar, V. (2008). Studies on crystal growth, vibrational and optical properties of organic nonlinear optical crystal: p-Aminoazobenzene, *Spectrochimica Acta Part A: Molecular and Biomolecular Spectroscopy*, C 71, 502-507.

[19] Varsányi, G., (1974). *Assignments for vibrational spectra of seven hundred benzene derivatives*, Halsted Press,

[20] Krishnakumar, V. and Prabavathi, N. (2008). Simulation of IR and Raman spectral based on scaled DFT force fields: a case study of 2-amino 4-hydroxy 6-trifluoromethylpyrimidine, with emphasis on band assignment, *Spectrochimica Acta Part A: Molecular and Biomolecular Spectroscopy*, C 71, 449-457.

[21] Altun, A., Gölcük, K., and Kumru, M. (2003). Structure and vibrational spectra of p-methylaniline: Hartree-Fock, MP2 and density functional theory studies, *Journal of Molecular Structure: THEOCHEM*, C 637, 155-169.

[22] Krishnakumar, V. and Xavier, R.J. (2003). Normal coordinate analysis of vibrational spectra of 2-methylindoline and 5-hydroxyindane.

[23] Seshadri, S., Gunasekaran, S., and Muthu, S. (2009). Vibrational spectroscopy investigation using density functional theory on 7-chloro-3-methyl-2H-1, 2, 4-benzothiadiazine 1, 1-dioxide, *Journal of Raman Spectroscopy: An International Journal for Original Work in all Aspects of Raman Spectroscopy, Including Higher Order Processes, and also Brillouin and Rayleigh Scattering*, C 40, 639-644.

[24] Anbarasu, P. and Arivazhagan, M. (2011). Scaled quantum chemical study of structure and vibrational spectra of 5-fluro-2-hydroxyacetophenone.

[25] Sundaraganesan, b.N., Ilakiamani, S., Saleem, H., Wojciechowski, P.M., and Michalska, D. (2005). FT-Raman and FT-IR spectra, vibrational assignments and density functional studies of 5-bromo-2-nitropyridine, *Spectrochimica Acta Part A: Molecular and Biomolecular Spectroscopy*, C 61, 2995-3001.

[26] Krishnakumar, V. and Mathammal, R. (2009). Density functional and experimental studies on the FT-IR and FT-Raman spectra and structure of benzoic acid and 3, 5-dichloro salicylic acid, *Journal of Raman Spectroscopy: An International Journal for Original Work in all Aspects of Raman Spectroscopy, Including Higher Order Processes,*

and also Brillouin and Rayleigh Scattering, C 40, 264-271.

[27] George, S. (2001). Infrared and Raman characteristic group frequencies: tables and charts, *Wiley, New Jersey*, C.

[28] Krishnakumar, V. and Balachandran, V. (2005). FTIR and FT-Raman spectra, vibrational assignments and density functional theory calculations of 2, 6-dibromo-4-nitroaniline and 2-(methylthio) aniline, *Spectrochimica Acta Part A: Molecular and Biomolecular Spectroscopy*, C 61, 1811-1819.

[29] Rao, R.K. and Sundar, N.S. (1993). Vibrational spectra of 2-fluoro-5-nitro-, 2-fluoro-4-nitro-, 4-fluoro-2-nitro-and 5-fluoro-2-nitrotoluene, *Spectrochimica Acta Part A: Molecular Spectroscopy*, C 49, 1691-1693.

[30] Mubarika, S., Gandjar, I.G., Hamann, M.T., Rao, K., and Wahyuono, S. (2005). Phalerin, a new benzophenoic glucoside isolated from the methanolic extract of Mahkota Dewa [Phaleria macrocarpa (scheff). Boerl.] leaves, *Indonesian Journal of Pharmacy*, C, 51-57.

[31] Jag, M. (2000). Organic spectroscopy: principles and applications.

[32] Bowman, W.D. and Spiro, T.G. (1980). MNDO–MOCIC evaluation of the uracil force field: Application to the interpretation of flavin vibrational spectra, *The Journal of Chemical Physics*, C 73, 5482-5492.

[33] Sundaraganesan, N. and Joshua, B.D. (2007). Vibrational spectra and fundamental structural assignments from HF and DFT calculations of methyl benzoate, *Spectrochimica Acta Part A: Molecular and Biomolecular Spectroscopy*, C 68, 771-777.

[34] Watanabe, T., Ebata, T., Tanabe, S., and Mikami, N. (1996). Size-selected vibrational spectra of phenol-(H2O) n (n= 1–4) clusters observed by IR–UV double resonance and stimulated Raman-UV double resonance spectroscopies, *The Journal of Chemical Physics*, C 105, 408-419.

[35] Coates, J. (2006). Interpretation of infrared spectra, a practical approach, *Encyclopedia of analytical chemistry: applications, theory and instrumentation*, C.

[36] Ahmad, S., Mathew, S., and Verma, P. (1992). Laser Raman and FT-infrared spectra of 3, 5-dinitrobenzoic acid, *Indian journal of pure & applied physics*, C 30, 764-765.

[37] Van der Maas, J. and Lutz, E.T.G. (1974). Structural information from OH stretching frequencies monohydric saturated alcohols, *Spectrochimica Acta Part A: Molecular Spectroscopy*, C 30, 2005-2019.

[38] Kurban, M. and Gündüz, B. (2018). Electronic structure, optical and structural properties of organic 5, 5′-Dibromo-2, 2′-bithiophene, *Optik*, C 165, 370-379.

[39] Mamand, D. Determination the band gap energy of poly benzimidazobenzophenanthroline and comparison between HF and DFT for three different basis sets, *Journal of Physical Chemistry and Functional Materials*, C 2, 31-35.

[40] Orek, C., Gündüz, B., Kaygili, O., and Bulut, N. (2017). Electronic, optical, and spectroscopic analysis of TBADN organic semiconductor: Experiment and theory, *Chemical Physics Letters*, C 678, 130-138.